Eur. Phys. J. **B15** (2000) 423-434

cond-mat/9910318
ETH-TH/99-27

A Spin-$\frac{1}{2}$ Model for $CsCuCl_3$ in an External Magnetic Field

A. Honecker[1ab], M. Kaulke[2,3], and K.D. Schotte[2,4]

[1] Institut für Theoretische Physik, ETH-Hönggerberg, CH–8093 Zürich, Switzerland, e-mail: a.honecker@tu-bs.de
[2] Fachbereich Physik, Freie Universität Berlin, Arnimallee 14, D–14195 Berlin, Germany
[3] e-mail: kaulke@physik.fu-berlin.de
[4] e-mail: schotte@physik.fu-berlin.de

October 19, 1999; revised December 28, 1999

Abstract. $CsCuCl_3$ is a ferromagnetically stacked triangular spin-1/2 antiferromagnet. We discuss models for its zero-temperature magnetization process. The models range from three antiferromagnetically coupled ferromagnetic chains to the full three-dimensional situation. The situation with spin-1/2 is treated by expansions around the Ising limit and exact diagonalization. Further, weak-coupling perturbation theory is used mainly for three coupled chains which are also investigated numerically using the density-matrix renormalization group technique. We find that already the three-chain model gives rise to the plateau-like feature at one third of the saturation magnetization which is observed in magnetization experiments on $CsCuCl_3$ for a magnetic field perpendicular to the crystal axis. For a magnetic field parallel to the crystal axis, a jump is observed in the experimental magnetization curve in the region of again about one third of the saturation magnetization. In contrast to earlier spinwave computations, we do not find any evidence for such a jump with the model in the appropriate parameter region.

PACS. 75.10.Jm Quantized spin models – 75.45.+j Macroscopic quantum phenomena in magnetic systems – 75.50.Ee Antiferromagnetics

1 Introduction

$CsCuCl_3$ is in several respects a quite unusual stacked triangular (anti)ferromagnet (see e.g. [1] for a review of the subject). Among others, three-dimensional features are vital in this compound: The ferromagnetic stacking is just an order of magnitude larger than the antiferromagnetic in-plane coupling while in most other materials the coupling constants differ at least by two orders of magnitude. Furthermore, the smaller antiferromagnetic coupling is crucial since it gives rise to a non-trivial behaviour of $CsCuCl_3$ in the presence of an external magnetic field.

The behaviour of $CsCuCl_3$ in strong external magnetic fields and at low temperatures has been studied already some time ago (see e.g. [2]). One observes different behaviour, depending on whether the magnetic field is applied along or perpendicular to the c (crystal)-axis. For a magnetic field along the c-axis, there is a jump in the magnetization curve at values of the magnetization of about one third of the saturation value. In contrast, one finds a plateau in the same area if the magnetic field is applied perpendicular to the c-axis[1].

The spin in $CsCuCl_3$ is carried by Cu^{2+} ions and thus is a spin 1/2. So, a proper treatment of quantum fluctuations is important. However, in order to be able to treat the three-dimensional situation, most theoretical approaches have so far been either phenomenological [4–6] or used first-order spinwave theory [7–10,5].

The goal of the present paper is to treat directly a spin-1/2 model with realistic XXZ-anisotropies. We will use series expansions around the Ising limit, numerical diagonalization and degenerate second-order weak-coupling perturbation theory.

When one solves a classical or Ising-version of this model, it becomes clear that essential features are already captured by a three-chain variant. The bulk of our paper will therefore concentrate on three antiferromagnetically coupled ferromagnetic chains. The simplification to a one-dimensional situation also opens the possibility of applying methods which work particularly well in one dimension like the density-matrix renormalization group (DMRG) method [11,12].

[a] A Feodor-Lynen fellow of the Alexander von Humboldt-foundation

[b] Present address: Institut für Theoretische Physik, TU Braunschweig, Mendelssohnstr. 3, D–38106 Braunschweig, Germany

[1] Actually, a plateau with $\langle M \rangle = 1/3$ can also be observed in other triangular antiferromagnets (see e.g. [3] for recent rather clear examples).

The purpose of the present paper is to gain some qualitative insight and demonstrate that new theoretical approaches to $CsCuCl_3$ are viable. It should be possible to develop all these approaches further to improve the accuracy of the results, to obtain a more realistic modeling or to compute other quantities.

2 The model

Now we proceed to give a more accurate description of our model and the parameter region we are interested in. We model $CsCuCl_3$ by a stacked triangular lattice antiferromagnet as sketched in Fig. 2.1.

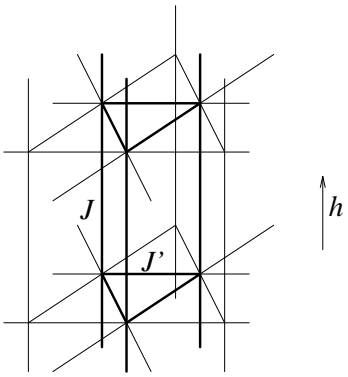

Fig. 2.1. The stacked triangular (anti)ferromagnet in a magnetic field h. The bold lines denote our three-chain model.

The quantum-spin Hamiltonian corresponding to Fig. 2.1 is given by (compare also [8]):

$$H = J\sum_{i=1}^{N}\sum_{x=1}^{L} \Delta_1 S^z_{i,x}S^z_{i,x+1} + \tfrac{1}{2}\left(S^+_{i,x}S^-_{i,x+1} + S^-_{i,x}S^+_{i,x+1}\right) + J'\sum_{\langle i,j\rangle}\sum_{x=1}^{L} \Delta_2 S^z_{i,x}S^z_{j,x} + \tfrac{1}{2}\left(S^+_{i,x}S^-_{j,x} + S^-_{i,x}S^+_{j,x}\right) - h\sum_{i,x} S^z_{i,x}\,, \qquad (2.1)$$

where the $\mathbf{S}_{i,x}$ are spin-1/2 operators and h is a dimensionless magnetic field. The notation $\langle i,j\rangle$ denotes neighbouring pairs of the N chains. Here, the number of chains N will be kept fixed while we are interested in the limit of infinite L. Mostly, we choose $\Delta_1 = \Delta_2$ and then denote both of them just by 'Δ'.

Quite often, $CsCuCl_3$ is modeled by a Hamiltonian which includes a Dzhalozhinski-Moriya interaction with a vector pointing along the ferromagnetic chains in order to account for a modulation in the magnetic structure with a period of slightly more than 70 layers along the c-axis [13]. However, by a local unitary transformation this can be traded for a contribution to the anisotropy Δ_2 and a surface term which is then discarded (see e.g. [8]). Further contributions to the anisotropies come from crystal fields. In this way, the z-direction in spin space is identified with the direction along the ferromagnetic chains (the c-axis) in real space.

J will be ferromagnetic ($J < 0$) and J' antiferromagnetic ($J' > 0$). In order to describe the material $CsCuCl_3$ one uses $J' \approx -J/6$ and Δ slightly less than one [14–17]. The actual values used should not matter so much; it should however be noted that $CsCuCl_3$ is described by weakly coupled ferromagnetic chains – though not so weakly coupled as is the case for many other triangular lattice antiferromagnets [1]. A Monte-Carlo simulation of an XY–model takes $J' = -J/10$ [18] showing the influence the weaker coupling has on the critical behaviour of triangular antiferromagnets. To make the situation clearer in the study of the few-chain problem we choose a bit stronger interchain coupling, e.g. $J' = -J/3$ to compensate partially for the missing neighbouring chains.

The $\langle i,j\rangle$-summation in (2.1) should run over a triangular lattice as sketched in Fig. 2.1. However, since $J' \ll |J|$, a reasonable first approximation should be obtained by retaining only one site as a representative for each of the three sublattices of the triangular lattice. This leads to the model of three coupled chains which is indicated by the bold lines in Fig. 2.1.

Since we are interested in the behaviour of $CsCuCl_3$ at low temperatures, we actually simplify to zero temperature in the present paper. We further restrict to magnetic fields applied along the anisotropy axis. The magnetization

$$\langle M\rangle = \frac{2}{NL}\left\langle \sum_{i=1}^{N}\sum_{x=1}^{L} S^z_{i,x}\right\rangle \qquad (2.2)$$

is then given as the expectation value of a conserved operator. This is technically useful since it permits one to relate all quantities in a magnetic field h to those with a given magnetization $\langle M\rangle$ at zero field. In the presence of an anisotropy $\Delta \neq 1$, the effect of a magnetic field along the z-axis is different from a magnetic field in the xy-plane. Because of the aforementioned simplification we consider only the former case in the present paper.

Possible plateaux in the magnetization curve can be most easily read off in the strong-coupling limit $J' \gg |J|$. For a fixed number N of coupled chains one finds [19, 20] that for $J = 0$ the only possible values of the magnetization are $\langle M\rangle = -1,\ -1+2/N,\ ...,\ 1-2/N,\ 1$. In particular, for all N that are divisible by three, a plateau with $\langle M\rangle = 1/3$ is possible (the simplest case is $N = 3$). However, this strong-coupling argument does not ensure that a certain plateau actually does occur for given values of the parameters – this issue requires a computation of the magnetization curve (at least in the vicinity of the plateau-value of the magnetization).

Before we proceed with the discussion of the magnetization process, we note that a straightforward computation yields the upper critical field for $N = 3$ cyclically coupled chains

$$h_{uc} = J'(\Delta_2 + \tfrac{1}{2}) + J(\Delta_1 - 1) \qquad (2.3)$$

for $J' > 0$ and $J < 0$. This result is based on the assumption that the transition proceeds with a single spin

flip and is therefore valid for Δ_1 small enough (in particular $\Delta_1 \leq 1$). If the transition to saturation becomes first order, (2.3) ceases to be valid.

3 Ising expansions for three chains

The Ising limit of $N = 3$ ferromagnetic chains (2.1) which are mutually antiferromagnetically coupled is easily understood: At zero temperature, only states with $\langle M \rangle = \pm 1$ and $\langle M \rangle = \pm 1/3$ are realized. The groundstate at $\langle M \rangle = 1/3$ is given by a configuration in which all spins in two chains point up and those in the third chain point down. Perturbation expansions in Δ^{-1} around this state and the ones with a single spin flipped respectively to it are readily performed. One finds the lowest gaps for the single spin excitations with states that are translational invariant along the chain direction, and antisymmetrized between the two equivalent chains for an additional spin flipped down.

With this information one proceeds in the same way as for the triangular lattice [21] (the precise method has been summarized in [22]) to find sixth-order series for the gap of a single flipped spin. The series for general J and J' can be found in appendix A. Here we just present the specialization to $J' = -J/3$:

$$\frac{h_{c_1}}{|J|} = -\Delta + \frac{7}{6} - \frac{11}{432\Delta^2} + \frac{1993}{72576\Delta^3} - \frac{5843545}{109734912\Delta^4} + \frac{202825209149}{2824576634880\Delta^5} + \mathcal{O}(\Delta^{-6}) , \tag{3.1}$$

$$\frac{h_{c_2}}{|J|} = \frac{4\Delta}{3} - 1 - \frac{1}{36\Delta} + \frac{11}{432\Delta^2} - \frac{3887}{54432\Delta^3} + \frac{1558903}{18289152\Delta^4} - \frac{33098775077}{224682232320\Delta^5} + \mathcal{O}(\Delta^{-6}) . \tag{3.2}$$

It should be noted that for sufficiently large Δ it is actually favourable to flip large clusters of spins rather than a single one if one changes the applied magnetic field. Therefore, the transition at large Δ is first order and (3.1) and (3.2) (or (A.1) and (A.2)) are not the boundaries of the $\langle M \rangle = 1/3$ plateau. Nevertheless, in contrast to other Ising series such as those for the triangular lattice [21], these series are remarkably well behaved down into the region $\Delta \approx 1$ for the values of parameters we are interested in (J' small). The ending point of the $\langle M \rangle = 1/3$ plateau is determined by the condition $h_{c_2}(\Delta_c) - h_{c_1}(\Delta_c) = 0$. For example, for $J'/|J| = 1/3$ we can use the raw series (3.1) and (3.2) and find that the plateau ends at $\Delta_c = 0.965$, 0.876 or 0.997 if one truncates the series at fourth, fifth or sixth order, respectively. At $J'/|J| = 1/6$ convergence is a bit better and using (A.1) and (A.2) one finds the ending point at $\Delta_c = 0.972$, 0.954 and 0.985 for fourth, fifth and sixth order, respectively.

This already indicates that the precise value of the XXZ-anisotropy is crucial for explaining the presence or absence of a plateau with $\langle M \rangle = 1/3$.

4 Exact diagonalization for three chains

Next we present exact diagonalization results for three cylindrically coupled chains with length $L = 8$. Fig. 4.1 shows the magnetic phase diagram for the $su(2)$-symmetric situation $\Delta = 1$. The lines show the magnetic fields at which a transition occurs between the states with the magnetization indicated in the figure (for $L = 8$, only $\langle M \rangle = m/12$ with $m = -12, \ldots, 12$ can be realized). One observes a plateau with $\langle M \rangle = 1/3$ for all $J' > 0$. The transition to saturation clearly is given by $h_{uc} = \frac{3}{2}J'$, as it should be according to (2.3). In the ferromagnetic regime $J' < 0$, the magnetization jumps from $\langle M \rangle = -1$ to $\langle M \rangle = 1$ as h passes through zero.

We would like to remark the striking smoothness of the transition lines in the weak-coupling regime $J' \ll |J|$ in Fig. 4.1. This suggests that expansions in J' should be a viable way to understand the magnetization process of three coupled chains (at least in a situation with some $su(2)$ symmetry preserved). This will be the subject of a later section.

For $J' \gg |J|$, we can use the effective Hamiltonian given in [19] to determine the lower boundary of the $\langle M \rangle = 1/3$ plateau. By exact diagonalization we find with $\Delta = 1$ that $h_{c_1}/|J| = 0.42096, 0.41880, 0.41779, 0.41723, 0.41689$ for $L = 8, 10, 12, 14, 16$, respectively, and in the limit $J/J' \to 0$. By comparison with Fig. 4.1 we see that the lower boundary of the $\langle M \rangle = 1/3$ plateau must therefore still increase beyond the right boundary of the figure.

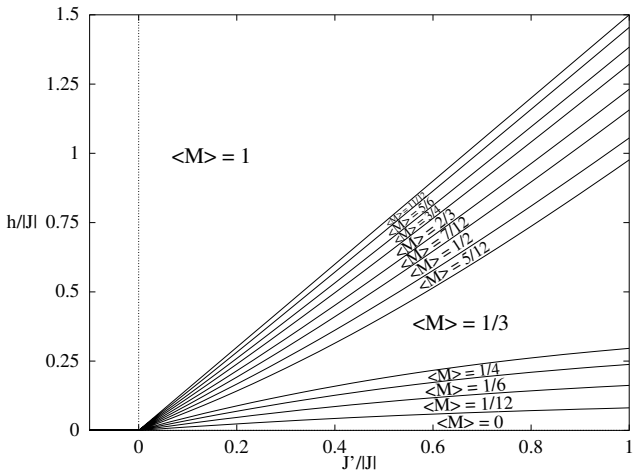

Fig. 4.1. Magnetic phase diagram for three coupled chains with $L = 8$ and $\Delta = 1$.

Now we fix the coupling constants to $J' = |J|/3$ and look at the dependence on the XXZ-anisotropy Δ. The resulting magnetic phase diagram for $L = 8$ is shown in Fig. 4.2.

One observes that for $\Delta \gtrsim 1.14$ only the values $\langle M \rangle = \pm 1/3$, ± 1 occur. The corresponding plateaux are separated by first-order transitions in this region. Outside this region, the lower boundary of the $\langle M \rangle = 1/3$ plateau and the transition to saturation seem to remain second-order

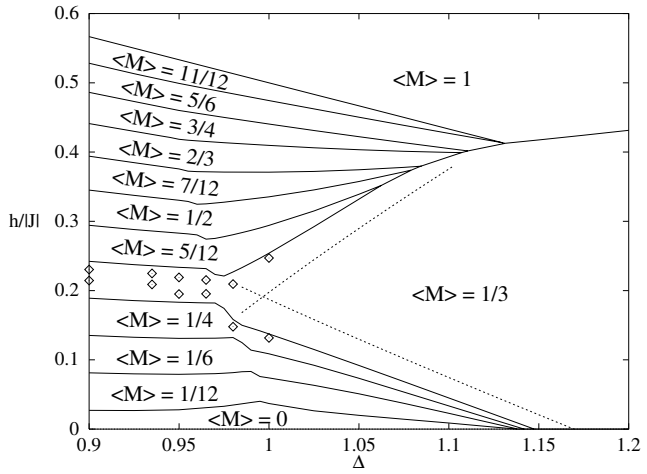

Fig. 4.2. Magnetic phase diagram for three coupled chains with $L = 8$ and $J' = |J|/3$. The dashed lines denote the sixth-order series (3.1) and (3.2). The diamonds denote extrapolated values of the boundary of the $\langle M \rangle = 1/3$ plateau (see next section).

transitions. The transition to saturation is given by (2.3) in the region where it is of second order.

The $\langle M \rangle = 1/3$ plateau can be observed in Fig. 4.2 for $\Delta \gtrsim 0.98$, *i.e.* it survives a small amount of XY-like anisotropy. The transition at its upper boundary becomes first order for weak Ising-like anisotropies. For $L = 8$ flipping two spins is favoured over flipping just one for $\Delta \gtrsim 1.05$. A guess about what happens in the thermodynamic limit $L \to \infty$ is not obvious. Furthermore, in the vicinity of $\Delta \approx 1.13$ there is some evidence for a jump in the magnetization curve at $h = 0$.

The dashed lines in Fig. 4.2 show the series expansions (3.1) and (3.2) in Δ^{-1}. They denote the energy-cost to flip a *single* spin above the $\langle M \rangle = 1/3$ plateau and should therefore be compared to the corresponding full lines. The agreement of these sixth-order series with the numerical data is quite good in view of the fact that the window shown in the figure is rather far from the regime $\Delta \to \infty$ where the series were derived. These series point to a closing of the plateau in about the same region indicated by the numerical data.

We conclude this section by noting that the transition to full magnetization is compatible with the Dzhaparidze-Nersesyan–Pokrovsky-Talapov (DN-PT) universality class [23,24]. From a technical point of view, it is important that conservation of the magnetization M reduces the dimension of the space of states considerably such that we can apply the exact diagonalization technique to large lattices. Actually, for many purposes it is sufficient to consider only two-spin deviations [25] which can be easily treated numerically for volumes of around 1000 spins. Nevertheless, for $J < 0$ one observes much stronger crossover effects than for $J > 0$ [20].

5 DMRG

Because of the one-dimensional topology of the three-leg ladder we have used DMRG [11] (for a detailed review of the DMRG method see also [12]) in order to determine more accurately the value of the anisotropy Δ where the plateau in the magnetization occurs. Similar DMRG computations for the magnetization process of a three-chain model with $J > 0$ have been carried out in [26,27] (see also [28] for a DMRG study of other spin ladders in a magnetic field). Details on our implementation of the DMRG procedure can be found in appendix B.

To do the calculations, three spins $\mathbf{S}_{i,x}$, $i = 1, 2, 3$ for fixed x (one triangle in Fig. 2.1) were combined to one site. In this way one ends up with a spin chain of L sites. We have calculated the $\langle M \rangle = 1/3$ plateau for ladders of 90 spins (30 sites in the corresponding chain model) for different values of the anisotropy Δ.

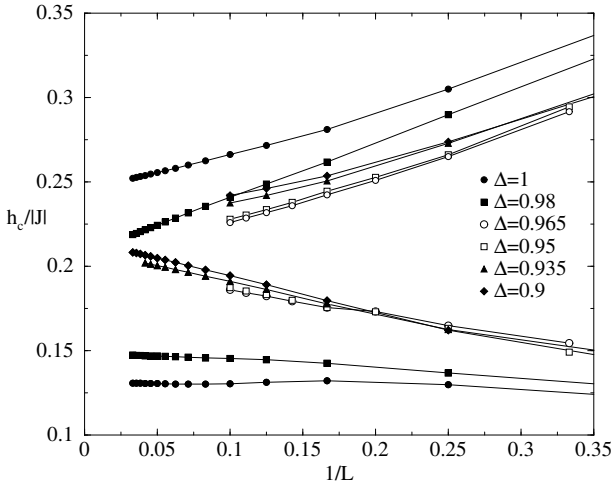

Fig. 5.1. Upper and lower critical fields as a function of $1/L$ for different values of Δ. Filled symbols denote DMRG results and open symbols data from exact diagonalization.

Fig. 5.1 shows the upper and lower critical fields as a function of the inverse chain length $1/L$. For large Δ (≥ 0.98) the $\langle M \rangle = 1/3$ plateau also exists in the thermodynamic limit. In the case of small Δ (≤ 0.935) the data is compatible with a vanishing plateau[2]. For $\Delta \leq 0.8$ the plateau width follows a $1/L$ law to a good approximation (this form is a strong indication of a vanishing plateau width).

The interesting point is the threshold where the plateau opens. However, the infinite-system algorithm of the DMRG method fails already for short chain lengths when Δ approaches the region around 0.95 where the threshold is expected. The reason for this is not yet clear. Therefore in Fig. 5.1 results from exact diagonalization are plotted

[2] Variation of the truncation level in the DMRG procedure indicates that the data may have errors up to $10^{-3}J \ldots 10^{-2}J$ for the larger system sizes.

for these values of Δ. The finite-size data for the plateau-boundaries has been extrapolated to infinite L using either a polynomial fit in $1/L$ or a fit with corrections of the form $\exp(-cL)$. The former fit should work well for small Δ while the latter one is justified when a plateau is present, *i.e.* for the larger values of Δ. The results of the extrapolation are shown by the diamonds in Fig. 4.2. The error of the extrapolation is smaller than the size of the symbols, but there are additional systematic errors (e.g. in the DMRG truncation procedure) which may be somewhat larger. Therefore, all the data taken together indicates that the plateau closes indeed at $\Delta \approx 0.95$ – at least it becomes unobservable in this region and for all practical purposes can be considered to be absent for $\Delta < 0.95$.

6 Weak-coupling expansions

Since the coupling constants for $CsCuCl_3$ lie in the weak-coupling regime $J' \ll |J|$, it is natural to try to analyze (2.1) by an expansion in J' around the decoupled point $J' = 0$. Such an approach is even more strongly suggested by Fig. 4.1 which shows that at least for $N = 3$ and $\Delta = 1$, the transition lines are very smooth functions of $J'/|J|$.

6.1 First order

We choose $\Delta_1 = 1$ in (2.1) for the weak-coupling expansions because of two reasons (Δ_2 will however be retained as a parameter). Firstly, we can then exploit the $su(2)$ symmetry of the decoupled chains in order to immediately write down their groundstates for a given magnetization. Secondly, in this case we can expect a smooth dependence on the coupling J' (see Fig. 4.1), which is not present otherwise (this is indicated by numerical diagonalization – compare also Fig. 4.2). A consequence of this choice $\Delta_1 = 1$ is that a given magnetization can be arbitrarily distributed among the individual chains. This means that the groundstate is highly degenerate and one has to perform degenerate perturbation theory.

The groundstate space of a single $su(2)$-symmetric ferromagnetic Heisenberg chain of length L is the spin-$L/2$ representation. Thus, one can immediately write down the groundstate with a given total $\mathcal{S}^z$ eigenvalue m:

$$|j = L/2, m\rangle = \frac{1}{\sqrt{\mathcal{N}_{j,m}}} \left(\mathcal{S}^-\right)^{j-m} |j, j\rangle \,, \tag{6.1}$$

where $\mathcal{S}^-$ is the total step operator for a single chain. Here j denotes this spin and m the eigenvalue of the z-component of the total spin operator. The normalization $\mathcal{N}_{j,m}$ in (6.1) should be chosen such that all states $|j, m\rangle$ are normalized to one. Otherwise it is sufficient to know that the number of terms on the r.h.s. of (6.1) is $\binom{2j}{j-m}$.

Because of translational invariance one readily finds that

$$\langle j, m|S^z_{i,x}|j, m\rangle = \frac{1}{L}\langle j, m|\mathcal{S}^z|j, m\rangle = \frac{m}{L} = \frac{m}{2j} \,. \tag{6.2}$$

A simple combinatorial consideration further leads to

$$\begin{aligned} \langle j, m+1|S^+_{i,x}|j, m\rangle &= \frac{\sqrt{(j-m)(j+m+1)}}{2j} \,, \\ \langle j, m-1|S^-_{i,x}|j, m\rangle &= \frac{\sqrt{(j-m+1)(j+m)}}{2j} \,. \end{aligned} \tag{6.3}$$

Note that due to translational invariance the matrix elements (6.2) and (6.3) do not depend on the position of the spin-operator x. The summation over x in (2.1) therefore just yields a factor $L = 2j$.

In (6.2) and (6.3) one recognizes the matrix elements of the $\mathbf{J}$ operators of a spin-j $su(2)$-representation normalized by a factor $1/(2j)$. Thus, the interaction part of the Hamiltonian (2.1) can be rewritten in first order as

$$H_I = \frac{J'}{2j} \sum_{\langle k,l\rangle} \Delta_2 J^z_k J^z_l + \tfrac{1}{2}\left(J^+_k J^-_l + J^-_k J^+_l\right) - h \sum_k J^z_k \,. \tag{6.4}$$

This form is particularly useful for an analytical treatment. Firstly, one sees that for $L = 2j \to \infty$, the first-order interaction maps to a problem of classical spins where each spin stands for one chain. In the groundstate of a classical spin model on the triangular lattice, all spins on one sublattice point in the same direction. Therefore, a triangular arrangement of ferromagnetic chains and three coupled chains become equivalent at first order in J' – only the coupling constant is rescaled by the different coordination number.

Using this mapping to a classical spin model, a number of conclusions can be drawn which apply to three coupled chains as well as the full triangular arrangement:

1. The entire magnetization curve is linear at $\Delta_2 = 1$.
2. For $\Delta_2 > 1$, the magnetization jumps from $\langle M\rangle = -m_0$ to $\langle M\rangle = m_0$ with $m_0 = (\Delta_2 - 1)/(3(\Delta_2 + 1))$ as h passes through zero (see also Fig. 4.2).
3. For $\Delta_2 > 1$ there is a plateau with $\langle M\rangle = 1/3$. Its lower boundary is given by $h_{c_1} = zJ'/4$ where z is the number of nearest neighbours ($z = 2$ for three coupled chains and $z = 6$ for an underlying triangular lattice). The upper boundary is more difficult to determine analytically – a lower bound[3] is given by $h_{c_2} \geq z\Delta_2 J'/4$.
4. The asymptotic behaviour of $\langle M\rangle$ as a function of h is linear close to saturation or to the boundaries of the $\langle M\rangle = 1/3$ plateau:

$$\langle M\rangle - M_c \propto h - h_c \,. \tag{6.5}$$

With $N = 3$ chains, the first conclusion can actually be obtained for finite L using a different argument which is also useful for determining the groundstate degeneracy: For $\Delta_2 = 1$ and $N = 3$ one can further rewrite eq. (6.4) as

$$\begin{aligned} H_I = \frac{J'}{4j}\left(\mathbf{J}_1 + \mathbf{J}_2 + \mathbf{J}_3\right)^2 - \frac{3J'(j+1)}{4} \\ -h\left(J^z_1 + J^z_2 + J^z_3\right) \,. \end{aligned} \tag{6.6}$$

[3] The important point is that $h_{c_2} > h_{c_1}$ for $\Delta_2 > 1$.

This shows that the energy is a quadratic function of the total spin (or the magnetization $\langle M\rangle$). Therefore, all steps in the finite-size magnetization curve acquire equal width at $\Delta_2 = 1$. Also the groundstate degeneracy can be easily inferred from the representation (6.6). It is found to be maximal at $\langle M\rangle = 1/3$ where it is equal to $L+1$ and minimal at $\langle M\rangle = 0, 1$ where the groundstate is unique.

The treatment of the second order is going to be based on a numerical determination of the groundstate of the interaction H_I at $N = 3$ and finite L. It is then important that the groundstate should be non-degenerate at first order. This precludes an analysis of the second order for the case $\Delta_2 = 1$ where after treatment of the first order one is still left with large degeneracies. For $\Delta_2 \neq 1$, the groundstates with a given magnetization are at most twofold degenerate[4]. This twofold degeneracy is due to the spatial symmetries of the three-chain model which can be used to lift it completely (alternatively, such a two-fold degeneracy can be ignored since it does not affect the results). Thus, in particular the case we are mainly interested in, namely $\Delta_2 < 1$ is amenable to a numerical treatment up to the second order.

6.2 Second order

If one goes beyond the first order, one has to consider also excitations that are created by the interaction from the ferromagnetic groundstates (6.1). At second order, only a single spin can be flipped in each chain. To deal with the second order perturbation it is therefore sufficient to look only at spinwave states

$$|j,m,k\rangle = \frac{1}{\sqrt{\hat{\mathcal{N}}_{j,m}}} \sum_{x=1}^{L} \mathrm{e}^{ikx} S^-_{i,x} |j, m+1\rangle \tag{6.7}$$

with a suitable normalization factor $\hat{\mathcal{N}}_{j,m}$. This representation is useful because the states (6.7) are eigenstates of the Hamiltonian H_0 for a single chain

$$\left(H_0 - \frac{JL}{4}\right) |j,m,k\rangle = |J|\,(1-\cos(k))\,|j,m,k\rangle\,. \tag{6.8}$$

The computation of the matrix elements is now a bit more cumbersome than for the first order but follows the same lines of combinatorial considerations. In this manner one finds the following counterpart of (6.2) for $k \neq 0$:

$$\langle j,m,k|S^z_{i,x}|j,m,0\rangle = -\frac{\mathrm{e}^{-ikx}}{2j}\sqrt{\frac{(j-m)(j+m)}{2j-1}}\,. \tag{6.9}$$

[4] Still, for $\Delta_2 > 1$ there are excited states above the groundstate(s) for a given magnetization which have a gap which closes rapidly with increasing system size L. Therefore, depending on the chain length L, the magnetization and the numerical accuracy, groundstate degeneracies may appear to be threefold in the region $\Delta_2 > 1$.

The $k \neq 0$ generalization of (6.3) is found to be given by

$$\begin{aligned}
\langle j,m+1,k|S^+_{i,x}|j,m\rangle &= -\frac{\mathrm{e}^{-ikx}}{2j}\sqrt{\frac{(j-m-1)(j-m)}{2j-1}}\,,\\
\langle j,m-1,k|S^-_{i,x}|j,m\rangle &= \frac{\mathrm{e}^{-ikx}}{2j}\sqrt{\frac{(j+m-1)(j+m)}{2j-1}}\,.
\end{aligned} \tag{6.10}$$

With the matrix elements (6.9) and (6.10) one can now easily write down the matrix elements for the interaction between two chains. It should be noted that due to translational invariance, spinwave states with momenta k and $-k$ have to come in pairs (in other words: $\sum_x \mathrm{e}^{-i(k+k')x} = L\delta_{k+k',0}$). This leads to a cancellation of the phase factors in (6.9) and (6.10) and thus makes the matrix elements of the interaction k-independent. Then the k-summation can be pulled out from the second-order matrix. So, one obtains for the second-order contribution

$$\langle\psi_1|V\left(\frac{JLN}{4} - H_0\right)^{-1} V|\psi_1\rangle = \mathcal{E}^{-1}\langle\psi_1|H^\dagger_{II}H_{II}|\psi_1\rangle\,, \tag{6.11}$$

where $|\psi_1\rangle$ is the eigenstate of the first-order matrix H_I. The energy denominator is given by

$$\mathcal{E}^{-1} = -\frac{1}{2|J|}\sum_{\kappa=1}^{L-1}\frac{1}{1-\cos\left(\frac{2\pi\kappa}{L}\right)} = -\frac{(L-1)\,(L+1)}{12|J|}\,. \tag{6.12}$$

In order to write H_{II} in a compact form, we introduce operators E^z_i, $E^\pm_i$ acting in the groundstate space of the ith chain as

$$E^z_i|j,m\rangle = |j,m\rangle\,, \qquad E^\pm_i|j,m\rangle = |j,m\pm1\rangle\,. \tag{6.13}$$

Since the matrix elements of H_{II} do not depend on k one can identify all spaces spanned by $|j,m,k\rangle$ for a given k with that spanned by $|j,m\rangle$. Then H_{II} can be written as

$$\begin{aligned}
\frac{H_{II}}{J'} = \sum_{\langle i,l\rangle}\Bigg\{ &\Delta_2\frac{\sqrt{(j-m_i)(j+m_i)(j-m_l)(j+m_l)}}{2j(2j-1)}E^z_iE^z_l\\
&-\frac{\sqrt{(j-m_i-1)(j-m_i)(j+m_l-1)(j+m_l)}}{4j(2j-1)}E^+_iE^-_l\\
&-\frac{\sqrt{(j+m_i-1)(j+m_i)(j-m_l-1)(j-m_l)}}{4j(2j-1)}E^-_iE^+_l\Bigg\}\,.
\end{aligned} \tag{6.14}$$

Here the m_i denote the quantum numbers of the state on which H_{II} is acting. The combination $H^\dagger_{II}H_{II}$ appearing in (6.11) can be expressed by spin operators. In the isotropic case $\Delta_2 = 1$ a simple form can be found

$$\frac{H^\dagger_{II}H_{II}}{J'^2} = \sum_{\langle i,l\rangle}\frac{(\mathbf{J}_i\mathbf{J}_l)^2 - 2j(j-1)\mathbf{J}_i\mathbf{J}_l + j^3(j-2)}{4j^2(2j-1)^2} \tag{6.15}$$

which reduces for large chain length $L = 2j \gg 1$ to $\sum_{\langle i,l\rangle}(\mathbf{J}_i\mathbf{J}_l/j^2 - 1)^2/16$ that is to the exchange between two chains squared instead of the simple exchange in first order perturbation theory given by (6.4). The squared exchange has been used as a tool to take into account quantum or thermal fluctuations (see [5] and references therein).

So far, everything is valid for a general underlying lattice. Let us now comment on the results obtained from this second-order approach for three chains. For this case, one can easily determine the groundstate $|\psi_1\rangle$ of (6.4) numerically for L up to a few hundred when $\Delta_2 < 1$. For short chains, the first and second order expansion terms obtained from (6.4) and (6.11) compare favourably with a direct diagonalization of the Hamiltonian (2.1). However, the second-order corrections to the energy obtained from (6.11) behave as L^2 for large L. Alternatively, the second-order corrections to $h(\langle M\rangle)$ computed from these energies are proportional to L for long chains. This means that the radius of convergence shrinks rapidly to zero with increasing L. The additional factor L which limits the second-order weak-coupling approach for three coupled chains can be traced to the energy denominator (6.12) which is the main source of the system-size dependence.

With hindsight this divergence of the second order can be expected since a one-dimensional ferromagnet cannot be stable to a weak antiferromagnetic perturbation if the chain length is long. Second order perturbation theory connects only two chains, if one compares with contributions to the ground state energy $\propto J'^{3/2}$ one gets from a Holstein–Primakoff analysis for two ferromagnetic chains coupled antiferromagnetically one notices immediately the difficulties. Further in the limit of vanishing J', one would find a linear behaviour of the magnetization (6.5) in the thermodynmic limit. Now, if one takes this limit $L \to \infty$ at fixed $J' > 0$, the asymptotic DNPT square root behaviour$\langle M\rangle - M_c \propto \sqrt{|h - h_c|}$ which is characteristic for one dimension [23,24] has to be recovered. Such an abrupt change in the functional form is simply not compatible whith a convergent perturbation expansion in the thermodynmic limit. Only in three and higher dimensions, the functional behaviour (6.5) remains valid for the interacting quantum system (see section 7 of [21] and references therein). So, the second-order correction has a chance to be convergent only if the thermodynamic limit is taken in all three directions simultaneously. On the one hand, this is the case most relevant to $CsCuCl_3$. On the other hand, already determination of the first order groundstate involves the solution of a spin-$L/2$ problem on the triangular lattice. Then the numerical effort becomes much larger than in the three-chain model and one gains little by the perturbative treatment in comparison to a direct numerical treatment of the full problem (which will be carried out in section 8.2). Therefore, here we do not pursue evaluation of the second order for the full three-dimensional situation further.

7 Exact diagonalization results for six chains

Now we briefly look at the Hamiltonian (2.1) for $N = 6$ chains. The coupling of the nearest neighbour pairs $\langle i,j\rangle$ $(1 \le i,j \le 6)$ is specified by the lines in the following picture:

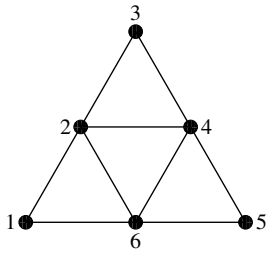

(7.1)

This is basically a refined version of the $N = 3$ chain model discussed in the preceding sections and thus a natural step in the direction of the three-dimensional compound. In particular, one can see that N must be a multiple of three if one wishes to expect a plateau with $\langle M\rangle = 1/3$ just on the basis of counting the chains. For $N = 6$, this counting argument indicates the possibility of having plateaux with $\langle M\rangle \in \{0, \pm 1/3, \pm 2/3, \pm 1\}$. If one now diagonalizes a single layer ($L = 1$) of the model specified by (2.1) and (7.1), one finds that all these values are indeed realized one after the other in the presence of a magnetic field.

In a way similar to section 4 we have computed the complete magnetization curve of this six-chain model for $L \le 4$ layers and parts of this curve for $L \le 35$ at two values $J'/|J| = 1/3$, $5/7$ and $\Delta = 1$ [5] The results for $3 \le L \le 6$ are shown in Fig. 7.1. The thick full lines in this figure are somewhat speculative extrapolations to $L = \infty$ which need discussion.

For all the sizes which we have investigated, there is an $\langle M\rangle = 0$ plateau (or equivalently a spin-gap), which however vanishes rapidly with increasing L. We are therefore confident that there is no $\langle M\rangle = 0$ plateau in the thermodynamic limit of the six-chain model, but rather a steep increase around $\langle M\rangle = 0$ as indicated by the thick full line in Fig. 7.1.

To see what happens to the other two plateaux which are permitted according to the aforementioned counting argument (*i.e.* $\langle M\rangle = 1/3$ and $\langle M\rangle = 2/3$) we have performed extrapolations of the available data for the boundaries of these plateaux using the vanden Broeck–Schwartz algorithm (see e.g. [29]). This works better for $\langle M\rangle = 2/3$ where we can use data for $2 \le L \le 6$ than for $\langle M\rangle = 1/3$ where just $L = 2, 3, 4$ is accessible. The result for $\langle M\rangle = 1/3$ is compatible with a plateau of zero width while for $\langle M\rangle = 2/3$ the error estimates indicate a non-vanishing plateau. The conclusion of the $\langle M\rangle = 1/3$ plateau being absent in the thermodynamic limit is further supported by the observation that at finite size this step is about as wide as the neighbouring ones. On the other hand, the

[5] The average coordination in the six-chain model (7.1) is larger than in the three-chain model which suggests to also investigate smaller J'. However, the data is already somewhat ambiguous at $J'/|J| = 1/3$. Therefore, we have added a larger value of J' rather than a smaller one.

width of the $\langle M \rangle = 2/3$ step is notably larger than that of its neighbours – at least for $J'/|J| = 5/7$.

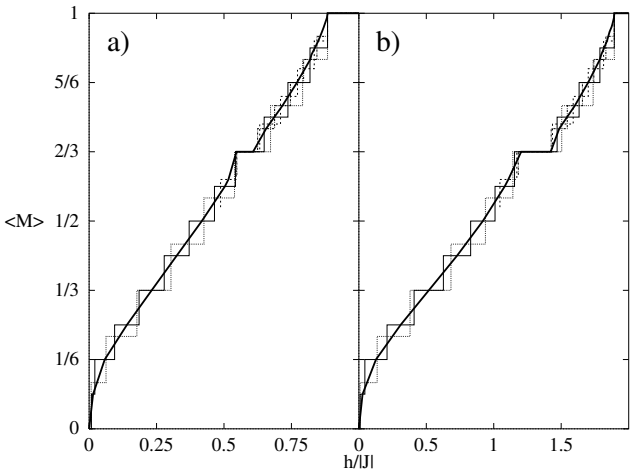

Fig. 7.1. Magnetization curves for six coupled chains with $\Delta = 1$ and a) $J'/|J| = 1/3$, b) $J'/|J| = 5/7$. The number of layers is $L = 3$ (dotted line), $L = 4$ (thin full line), $L = 5$ (dashed line) and $L = 6$ (dashed-dotted line). The thick full line is the extrapolation to $L = \infty$ discussed in the text.

Therefore we have decided to draw plateaux at $\langle M \rangle = 2/3$ in Fig. 7.1 but none for $\langle M \rangle = 1/3$. The boundaries of the former case are the only points where fairly reliable extrapolations to $L = \infty$ are available. Otherwise we follow the procedure of [30,31] and draw a line through the midpoints of the steps at the largest available system size, although it is apparent from Fig. 7.1 that finite-size effects are still of some importance.

Finally, the transition to saturation is of the same type as that for the three-leg ladder, *i.e.* it is again compatible with the DN-PT universality class [23,24], but subject to strong crossover effects in the region $J < 0$.

The main result of this discussion of $N = 6$ chains is that already doubling the number of chains leads to a vanishing of the $\langle M \rangle = 1/3$ plateau – at least for $\Delta = 1$ and weak coupling J'. This is a first indication that this plateau which is easily observable in $N = 3$ coupled chains might actually not survive the infinite-lattice limit in the plane perpendicular to the chains.

8 The three-dimensional case

The results from the various techniques which we have applied so far to simple models agree well with each other. This encourages us to proceed a bit further and look at the three-dimensional model corresponding to $CsCuCl_3$. This means we consider the Hamiltonian (2.1) where the nearest neighbour pairs $\langle i, j \rangle$ will now be those of the two-dimensional triangular lattice.

8.1 Ising expansions

We start with Ising expansions. The structure of the state with $\langle M \rangle = 1/3$ and the lowest single-spin excitations above it is readily inferred from the treatment of three coupled chains and the two-dimensional triangular lattice [21]. It is then straightforward to obtain fourth-order series for these excitation energies[6]. The explicit series can be found in appendix A. As before, these results correspond to the boundaries of the $\langle M \rangle = 1/3$ plateau for sufficiently small Δ. At large values of Δ, the associated transitions should be first order such that one would have to look at other excitations to determine these boundaries.

If we insert the value $J' = |J|/3$ into the raw fourth-order series (A.3,A.4) we find that the plateau closes at $\Delta_c = 0.939$. Using instead $J' = |J|/6$ (which is appropriate for $CsCuCl_3$), the ending point shifts to $\Delta_c = 0.948$. Both values are slightly smaller than those obtained for the three-chain model with the same order. However, in this region the actual values should not be taken too seriously, *i.e.* higher orders should still important and numerical data will indicate that the true Δ_c is probably larger. The main conclusion obtained from the Ising series is that the $\langle M \rangle = 1/3$ plateau closes in the region $\Delta_c \approx 1$, probably somewhere slightly below one in the region of XY-type anisotropies.

8.2 Exact diagonalization

To locate the ending point more accurately and to see if a jump in the magnetization curve develops, we have also numerically computed magnetization curves on three-dimensional $3 \times 3 \times L$ clusters. Some magnetization curves are shown in Fig. 8.1. Two criteria can be used to discuss the magnetization process in the region $\langle M \rangle = 1/3$:

1. If the magnetization curve passes smoothly through $\langle M \rangle = 1/3$, the width of the finite-size plateau at $\langle M \rangle = 1/3$ should scale as $1/L$ (with L the number of stacked segments of the triangular lattice).
2. For a smooth curve at magnetization $\langle M \rangle$, the neighbouring steps of the finite-size magnetization curves should have the same width. If a plateau is present, the step with magnetization $\langle M \rangle$ should be broader than its neighbours. A jump at sufficiently large system sizes should in contrast be indicated by a step that is smaller than its neighbours at small system sizes.

A remark is in order before we apply these criteria to our data. Although we expect to obtain a reasonable approximation to the thermodynamic limit despite the small linear size of the systems accessible to us, one can clearly not rule out that the behaviour would change on larger systems. Our conclusions should therefore be taken as a probable possibility.

For $J'/|J| = 1/6$ and $\Delta = 1$, both criteria indicate the presence of a small plateau with $\langle M \rangle = 1/3$. Instead for

[6] This can probably be pushed a bit further. Higher-order series have been computed numerically e.g. for the Heisenberg model on three-dimensional cubic lattices [32].

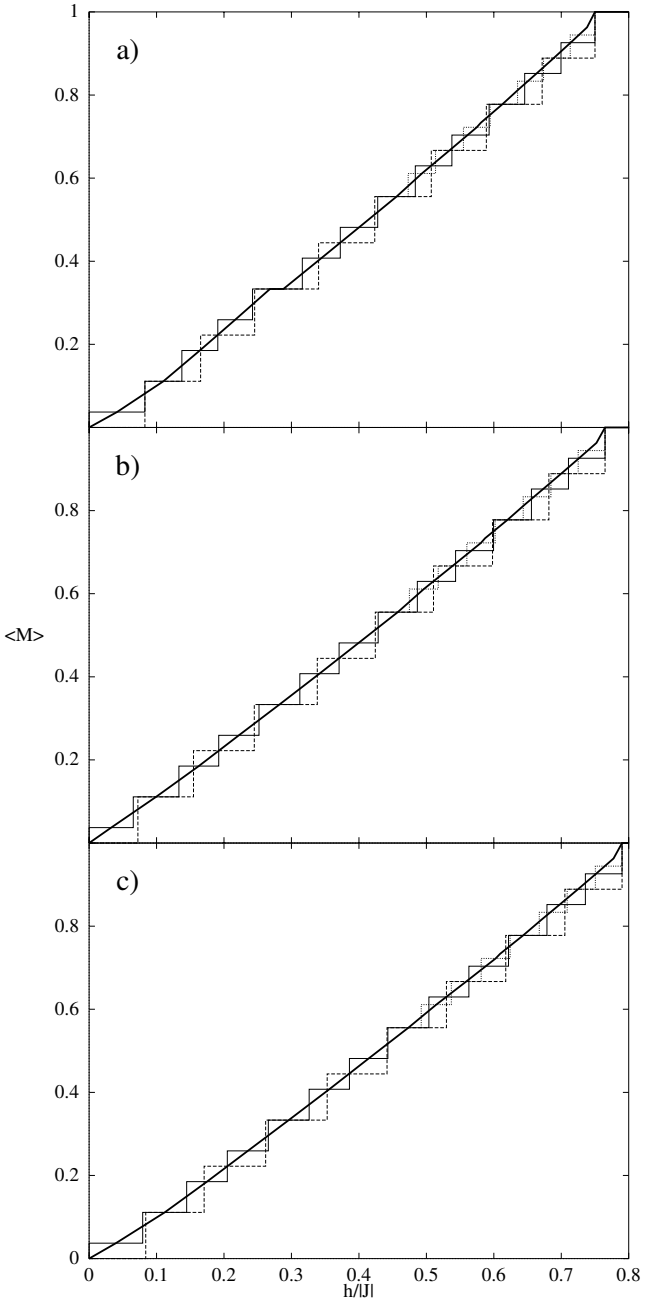

Fig. 8.1. Magnetization curves of $3 \times 3 \times L$ clusters with a) $J'/|J| = 1/6$, $\Delta = 1$; b) $J'/|J| = 1/6$, $\Delta = 0.97$; c) $J'/|J| = 0.172882193$, $\Delta_1 = 0.98789825$, $\Delta_2 = 1$. The number of layers is $L = 2$ (dashed line), $L = 3$ (thin full line) and $L = 4$ (dotted line). The bold full line is an extrapolation to $L = \infty$.

$J'/|J| = 1/6$ and $\Delta = 0.97$ both criteria applied to $L = 2$ and $L = 3$ point to a smooth magnetization curve in the region $\langle M \rangle = 1/3$. This suggests $1 > \Delta_c > 0.97$ which is slightly larger than that found from the fourth-order Ising expansions.

Since we did not find evidence for a jump so far, we also performed diagonalizations for the parameters $J'/|J| = 0.172882193$, $\Delta_1 = 0.98789825$, $\Delta_2 = 1$, since for these precise parameters a jump was found in [8] using first-order spinwave theory. The finite-size magnetization curves for these parameters are shown in Fig. 8.1c). Again, both criteria discussed above are compatible with a smooth curve at $\langle M \rangle = 1/3$, *i.e.* neither a plateau nor a jump seems to be present. However, on a system with volume $27 = 3 \times 3 \times 3$, we would expect some indication for a jump of size $\delta\langle M \rangle \approx 0.04$ as estimated in [8] or even $\delta\langle M \rangle \approx 0.01$ as observed experimentally [2]. One may attribute the absence of such signals for a jump to finite-size effects beyond the discretization of the magnetization curve at a volume with 27 spins. However, it can be seen at larger $\langle M \rangle$ that increasing the number of layers L leads only to small finite-size effects. On the other hand, also the approach of [8] is based on several approximations and is therefore not guaranteed to describe the situation with spin 1/2 accurately.

To conclude this section, let us briefly comment on the utility of order parameters which one might suspect to be useful for characterizing the transition. First, one could check numerically that the correct spin structures have been used in [8]. However, we do believe that the spin structures are indeed the umbrella-type and coplanar configurations in the low- and high-field regions, respectively. In fact, this has been reliably established via a mapping to a gas of hard-core bosons [33] for magnetic fields close to the saturation value. The question which we raised above regards the nature of the transition which occurs at intermediate fields, *i.e.* if it is second order, first order or occurs e.g. via an intermediate phase. However, we do not expect much additional insight into the nature of the transition from a numerical determination of order parameters, mainly because of finite-size effects such as the discretization of the magnetization axis. For this purpose the magnetization $\langle M \rangle$ (which we have discussed above) might even be somewhat better suited although it is not an order parameter.

9 Conclusions

We have theoretically observed a plateau with $\langle M \rangle = 1/3$ in a frustrated triangular magnet. For applications to $CsCuCl_3$, it is important to observe that the width of this plateau depends on several factors.

Consider for example a single triangle. If there are only three spin-1/2 spins, the magnetization can obviously only have the values $\langle M \rangle = \pm 1/3$ and ± 1. The plateau with $\langle M \rangle = 1/3$ survives (at least for $\Delta = 1$) the ferromagnetic stacking of infinitely many triangles, but the interaction reduces its width. A similar phenomenon occurs if one instead takes the limit of a two-dimensional triangular lattice in the plane. Also here, the plateau survives the thermodynamic limit for $\Delta \approx 1$ [34,21], but again gets narrower.

A further factor is the XXZ-anisotropy Δ. For a magnetic field along the c-axis, the plateau with $\langle M \rangle = 1/3$ survives only a small amount of XY-like anisotropy before it disappears. The same observation has already been made for the triangular lattice antiferromagnet [34,21]. If

the magnetic field is applied in the triangular plane perpendicular to the c-axis, an opposite behaviour is known from the triangular lattice antiferromagnet [35]: Here one observes a clear plateau-like feature in the region $\langle M\rangle = 1/3$ even in the XY case $\Delta = 0$.

If one combines these observations with the parameters which are appropriate for the description of $CsCuCl_3$, one understands the absence of a plateau for a magnetic field in the direction of the c-axis and that a plateau-like feature only occurs if the magnetic field is applied in the plane [2].

In contrast, we failed to reproduce the jump observed experimentally [2] for a magnetic field along the c-axis with the model (2.1) in the appropriate parameter region. While we observe several first-order transitions for $\Delta > 1$, we have no evidence for first-order transitions for $\Delta < 1$. Actually, our results for the three-chain model as well as similar ones for the two-dimensional triangular lattice [21] provide quite strong evidence against such a jump for spin 1/2 and $\Delta < 1$. However, a first-order spinwave analysis [8] predicted a jump in the magnetization curve of the Hamiltonian (2.1) with $\Delta_1 < 1$. Since it may be possible that this jump cannot occur in less than three dimensions, we have also investigated the three-dimensional spin-1/2 model numerically. Using precisely the same parameters as in [8], we did not find any evidence for a jump on $3\times3\times L$ clusters either. This discrepancy is puzzling, in particular since the weak-coupling analysis shows that weakly coupled ferromagnetic chains are close to a classical situation (though in two rather than in three dimensions[7]). While we cannot fully exclude that one would find a jump in the spin-1/2 model at larger system sizes, also the discussion in [8] is based on several approximations. We therefore believe that the issue of the experimentally observed jump deserves further theoretical attention. One possibility is also that this jump is caused by effects which are not incorporated into the model (2.1), such as elastic response to the external magnetic field. The anomalies observed in a recent soundwave propagation experiment [36] may be a further indication for the necessity of such extensions.

In summary, we have shown that a three-chain model describes the low-temperature magnetization process of $CsCuCl_3$ almost as well as the full three-dimensional model. The three-chain model has the advantage of being simpler to analyze. We have concentrated on zero (or small) temperature, but there is also a large amount of experimental data on the h-T phase diagram (see [37–39] for a small selection of recent results) which are waiting to be discussed in the framework of microscopic models. The three-chain model which we have discussed in the present paper may be a useful starting point since one should be able to treat it with a finite-temperature variant [40,41,12] of the DMRG procedure.

From a technical point of view, we have shown that the Hamiltonian (2.1) with spin 1/2 can be analyzed by several methods. Each of them has the potential of being pushed further to obtain more accurate results. This applies in particular to the weak-coupling approach: The second order diverges for the three-chain model as $L\to\infty$, but it remains to be investigated if it converges in three dimensions. The computation of other quantities than just the magnetization is also straightforward with each of the methods used in the present paper.

Useful discussions with D.C. Cabra, T. Nikuni, I. Peschel, P. Pujol, U. Schotte, H. Tanaka and M.E. Zhitomirsky are gratefully acknowledged. We are indebted to the Max-Planck-Institut für Mathematik, Bonn-Beuel and the C4 cluster of the ETH for allocation of CPU time.

[7] More precisely, each ferromagnetic chain can be regarded as one single spin with large S. It might therefore actually be interesting to try to treat our second-order expression in J' in three dimensions using spinwave techniques.

A Ising series

In this appendix we present explicit series in the Ising anisotropy Δ^{-1}.

For the $\langle M\rangle = 1/3$ plateau in the *three-chain model*, one finds the following sixth-order series for the gap of a single spin flipped up

$$\begin{aligned}
h_{c_2} = {} & \Delta\,(J'-J) + J + J'^2\Bigg\{\frac{1}{4J}\Delta^{-1} + \frac{5J'-2J}{16J^2}\Delta^{-2} \\
& + \frac{164J^2J'^2 - 258J^3J' + 276J^4 - 93J'^3J + 19J'^4}{192J^3\,(J'-J)\,(J'-2J)}\Delta^{-3} \\
& + \frac{\Delta^{-4}}{2304J^4\,(J'-J)^2\,(J'-2J)^2}\Big(19050J'^3J^4 \\
& \quad -8234J'^4J^3 + 3297J'^5J^2 - 27548J'^2J^5 \\
& \quad +20232J'J^6 - 1136J'^6J + 171J'^7 - 6480J^7\Big) \\
& + \frac{\Delta^{-5}}{55296\,(J'-2J)^3\,J^5\,(J'-3J)\,(J'-4J)\,(J'-J)^3} \\
& \quad \Big(62217652J'^4J^8 - 35026088J'^5J^7 \\
& \quad -76513096J'^3J^9 + 65015952J'^2J^{10} \\
& \quad +14995748J'^6J^6 - 7562886J'^7J^5 \\
& \quad +8581J'^{12} + 4998735J'^8J^4 - 2554610J'^9J^3 \\
& \quad +783380J'^{10}J^2 - 128008J'^{11}J \\
& \quad -35276256J^{11}J' + 9134208J^{12}\Big)\Bigg\} \\
& + \mathcal{O}(\Delta^{-6})\,. \qquad \text{(A.1)}
\end{aligned}$$

For an excitation with a single spin flipped down one finds instead the following sixth-order series

$$\begin{aligned}
h_{c_1} = {} & \Delta J - J + \frac{J'}{2} - J'^2\Bigg\{\frac{2J'-3J}{16J^2}\Delta^{-2} \\
& + \frac{47J^2J'^2 - 39J^3J' + 30J^4 - 25J'^3J + 5J'^4}{64J^3\,(J'-J)\,(J'-2J)}\Delta^{-3} \\
& + \frac{\Delta^{-4}}{4608J^4\,(J'-J)^2\,(J'-2J)^2}\Big(24218J'^3J^4
\end{aligned}$$

$$
\begin{aligned}
&-17776J'^4J^3+10901J'^5J^2-30028J'^2J^5\\
&+24264J'J^6-4054J'^6J+611J'^7-8784J^7\Big)\\
&+\frac{\Delta^{-5}}{110592\,(J'-J)^3\,(J'-4J)\,(J'-3J)\,J^5}\\
&\times\frac{1}{(J'-2J)^3\,(2J'-3J)}\Big(468904952J'^5J^8\\
&-400904412J'^6J^7-488731468J'^4J^9\\
&+415953144J'^3J^{10}-263997936J'^2J^{11}\\
&+309762362J'^7J^6-199502115J'^8J^5\\
&-23421312J^{13}+51214J'^{13}+111406752J^{12}J'\\
&+97003020J'^9J^4-32952968J'^{10}J^3\\
&+7259020J'^{11}J^2-923565J'^{12}J\Big)\Big\}\\
&+\mathcal{O}(\Delta^{-6})\,. \qquad \text{(A.2)}
\end{aligned}
$$

In a similar way, one obtains the following fourth-order series for the single-spin excitation above $\langle M\rangle = 1/3$ in the *three-dimensional model*

$$
\begin{aligned}
h_{c_1} &= J\Delta+\frac{3J'}{2}-J\\
&+\frac{3J'^3\left(9JJ'-10J^2+10J'^2\right)}{8\Delta\,(J'-J)\,(3J'-2J)\,(2J'-J)\,(J'-2J)}\\
&-\frac{3J'^2}{32\Delta^2\,(J'-2J)^2\,(2J'-J)^2\,(3J'-2J)\,(J'-J)^2}\\
&\Big(292J'^6-900JJ'^5+1203J^2J'^4-1222J^3J'^3\\
&+896J^4J'^2-344J^5J'+48J^6\Big)\\
&+\frac{J'^2}{256\Delta^3}\Big(3696796800J'^{18}-5988208896J'^3J^{15}\\
&+4368432498318J'^{12}J^6-3140479722337J'^{13}J^5\\
&-3154044909140J'^9J^9-41660867520J'^{17}J\\
&+30196054016J'^4J^{14}+221631078840J'^{16}J^2\\
&-117183492672J'^5J^{13}-742570973868J'^{15}J^3\\
&+362869230400J'^6J^{12}+1760559743358J'^{14}J^4\\
&-912414730048J'^7J^{11}+1875316243840J'^8J^{10}\\
&+4333067026982J'^{10}J^8-4842206323349J'^{11}J^7\\
&+854889984J'^2J^{16}-77524992J^{17}J'+3317760J^{18}\Big)\\
&\times\Big\{(J'-J)^3\,(3J'-2J)^3\,(2J'-J)^3\,(J'-2J)^3\\
&(3J'-4J)\,(5J'-4J)\,(4J'-3J)\,(5J'-3J)\\
&(4J'-J)\,(3J'-J)\,(5J'-2J)\Big\}^{-1}\\
&+\mathcal{O}(\Delta^{-4})\,, \qquad \text{(A.3)}
\end{aligned}
$$

and

$$
\begin{aligned}
h_{c_2} &= (3J'-J)\,\Delta+J-\frac{3J'^2\left(6J^2-11JJ'+10J'^2\right)}{4\Delta\,(J'-J)\,(2J'-J)\,(J'-2J)}\\
&+\frac{3J'^2\left(50J'^3-37JJ'^2-12J^2J'+12J^3\right)}{16\Delta^2\,(J'-2J)\,(2J'-J)\,(J'-J)^2}\\
&+\frac{J'^2}{64\Delta^3}\Big(13530240J'^{15}+80661600J'^2J^{13}\\
&-5086562914J'^9J^6+1224415456J'^4J^{11}\\
&-2716474016J'^5J^{10}+4432214446J'^6J^9\\
&-387107136J'^3J^{12}-5597333776J'^7J^8\\
&+5797552217J'^8J^7+3611625955J'^{10}J^5\\
&-1800747488J'^{11}J^4+447946876J'^{12}J^3\\
&+60036504J'^{13}J^2-70410816J'^{14}J\\
&-9897984J^{14}J'+539136J^{15}\Big)\\
&\times\Big\{(J'-2J)^3\,(J'-J)^3\,(3J'-2J)\,(3J'-4J)\\
&(5J'-4J)\,(4J'-3J)\,(2J'-J)^3\,(3J'-J)\\
&(5J'-3J)\,(4J'-J)\Big\}^{-1}\\
&+\mathcal{O}(\Delta^{-4})\,. \qquad \text{(A.4)}
\end{aligned}
$$

The results (A.3,A.4) are consistent with earlier ones. Firstly, for $J=0$, one recovers the series for the triangular lattice [21]. For general $J<0$ also (A.1) and (A.2) match with (A.4) and (A.3), respectively up to first order in J' (one just has to rescale J' by a factor 3 to account for the different coordination number).

B Details of the DMRG procedure

Following the standard infinite-size algorithm of the DMRG method [11], we enlarge the chain in each iteration step by two triangles (in total six spin-1/2 sites), *i.e.* by $8\times 8=64$ states. This is different from [26] where the totally antiferromagnetic case of the Hamiltonian (2.1) has been treated. There, the chain was built up by adding a total of only two spin-1/2 sites in each step, so that it took three DMRG steps to add two complete triangles to the original ladder. In this procedure more truncation operations of the Hilbert space had to be performed than in our calculation. But by adding eight-state sites in each step the number of basis states discarded in the truncation process is larger than in the case where only two-state sites are added. As far as we know it has not yet been tested which procedure is more favourable.

In order to limit the computational effort, we applied only the infinite-system algorithm even though more accurate results could probably be obtained when one would use in addition the finite-system algorithm. To calculate the boundaries of the magnetization plateau we have used spin conservation and performed three different calculations to target each of the groundstates with magnetization $\langle M\rangle = 1/3-1/S_{\rm tot},\, 1/3,\, 1/3+1/S_{\rm tot}$ separately. The difference between the groundstate energy in the sector $\langle M\rangle = 1/3$ and the energies in the neighbouring sectors

then gives the magnetic field:

$$h_{c1} = E_0\left(\langle M\rangle = \tfrac{1}{3} + \tfrac{1}{S_{\rm tot}}, L\right) - E_0\left(\langle M\rangle = \tfrac{1}{3}, L\right) \quad \text{(B.1)}$$

$$h_{c2} = E_0\left(\langle M\rangle = \tfrac{1}{3}, L\right) - E_0\left(\langle M\rangle = \tfrac{1}{3} - \tfrac{1}{S_{\rm tot}}, L\right). \quad \text{(B.2)}$$

Fig. B.1 shows a typical spectrum of the eigenvalues of the density matrix for such a calculation.

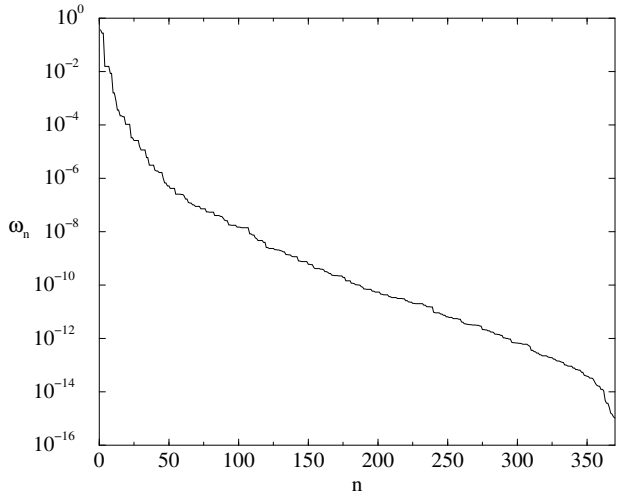

Fig. B.1. Eigenvalue spectrum of the reduced density matrix of a ladder with 24 spins ($L = 8$), calculated with 64 kept states in the subspace $\langle M\rangle = 1/3$. The couplings are $J = -1$, $J' = 1/3$ and $\Delta = 1$

The eigenvalues drop exponentially as is known from other quantum spin chains[8] and thus gives rise to a very small truncation error. On the other hand, we found that at least 160 states of the density matrix, *i.e.* 1280 states in one part of the chain had to be kept to obtain reliable results up to three decimal places in the energy. The eigenvalues of the density matrix lie about three to four orders of magnitude above the eigenvalues in the corresponding spectrum [46] of the totally antiferromagnetic case studied in [26]. This is one reason for the lower accuracy of our DMRG calculations. There is also a big difference between the truncation error and the real error in the groundstate energy which indicates that the structure of the groundstate could be approximated better by applying the finite-system algorithm.

References

1. M.F. Collins, O.A. Petrenko, Can. J. Phys. **75**, (1997) 605-655.
2. H. Nojiri, Y. Tokunaga, M. Motokawa, Journal de Physique **49**, Suppl. C8, (1988) 1459-1460.
3. T. Inami, Y. Ajiro, T. Goto, J. Phys. Soc. Jpn. **65**, (1996) 2374-2376.
4. E.P. Stefanovskiĭ, A.L. Sukstanskiĭ, JETP Lett. **57**, (1993) 294-298.
5. T. Nikuni, A.E. Jacobs, Phys. Rev. **B57**, (1998) 5205-5212.
6. A.E. Jacobs, T. Nikuni, J. Phys.: Condensed Matter **10**, (1998) 6405-6416.
7. H. Shiba, T. Nikuni, in *Recent Advance in Magnetism of Transition Metal Compounds*, A. Kotani, N. Suzuki (eds.), (World Scientific, Singapore 1993) 372-381.
8. T. Nikuni, H. Shiba, J. Phys. Soc. Jpn. **62**, (1993) 3268-3276.
9. A.E. Jacobs, T. Nikuni, H. Shiba, J. Phys. Soc. Jpn. **62**, (1993) 4066-4080.
10. E. Rastelli, A. Tassi, Phys. Rev. **B49**, (1994) 9679-9687; J. Appl. Phys. **75**, (1994) 6051-6053.
11. S.R. White, Phys. Rev. Lett. **69**, (1992) 2863-2866; Phys. Rev. **B48**, (1993) 10345-10356.
12. I. Peschel, X. Wang, M. Kaulke, K. Hallberg (eds.), *Density-Matrix Renormalization*, Lecture notes in physics 528 (Springer, Berlin 1999).
13. K. Adachi, N. Achiwa, M. Mekata, J. Phys. Soc. Jpn. **49**, (1980) 545-553.
14. H. Hyodo, K. Ijo, K. Nagata, J. Phys. Soc. Jpn. **50**, (1981) 1545-1550.
15. Y. Tazuke, H. Tanaka, K. Ijo, K. Nagata, J. Phys. Soc. Jpn. **50**, (1981) 3919-3924.
16. H. Tanaka, U. Schotte, K.D. Schotte, J. Phys. Soc. Jpn. **61**, (1992) 1344-1350.
17. M. Mekata, Y. Ajiro, T. Sugino, A. Oohara, K. Ohara, S. Yasuda, Y. Oohara, H. Yoshizawa, Journal of Magnetism and Magnetic Materials **140-144**, (1995) 1987-1988.
18. M.L. Plumer, A. Mailhot, J. Phys.: Condensed Matter **9**, (1997) L165-L170.
19. D.C. Cabra, A. Honecker, P. Pujol, Phys. Rev. Lett. **79**, (1997) 5126-5129.
20. D.C. Cabra, A. Honecker, P. Pujol, Phys. Rev. **B58**, (1998) 6241-6257.
21. A. Honecker, J. Phys.: Condensed Matter **11**, (1999) 4697-4713.
22. A. Honecker, J. Stat. Phys. **82**, (1996) 687-741.
23. G.I. Dzhaparidze, A.A. Nersesyan, JETP Lett. **27**, (1978) 334-337.
24. V.L. Pokrovsky, A.L. Talapov, Phys. Rev. Lett. **42**, (1979) 65-67.
25. R.P. Hodgson, J.B. Parkinson, J. Phys. C: Solid State Phys. **18** (1985) 6385-6395.
26. K. Tandon, S. Lal, S.K. Pati, S. Ramasesha, D. Sen, Phys. Rev. **B59** (1999) 396-410.
27. R. Citro, E. Orignac, N. Andrei, C. Itoi, S. Qin, preprint cond-mat/9904371.
28. R. Wießner, A. Fledderjohann, K.-H. Mütter, M. Karbach, Phys. Rev. **B60**, (1999) 6545-6551.
29. M. Henkel, G.M. Schütz, J. Phys. A: Math. Gen. **21**, (1988) 2617-2633.
30. J.C. Bonner, M.E. Fisher, Phys Rev. **135**, (1964) A640-658.
31. J.B. Parkinson, J.C. Bonner, Phys. Rev. **B32**, (1985) 4703-4724.
32. J. Oitmaa, C.J. Hamer, Z. Weihong, Phys. Rev. **B50**, (1994) 3877-3893.
33. T. Nikuni, H. Shiba, J. Phys. Soc. Jpn. **64**, (1995) 3471-3483.

[8] Although the number of applications of the DMRG has increased in the last few years, only a small amount of eigenvalue spectra of the used density matrices can be found in the literature. Some spectra are discussed in [11,42–45].

34. H. Nishimori, S. Miyashita, J. Phys. Soc. Jpn. **55**, (1986) 4448-4455.
35. N. Suzuki, F. Matsubara, Phys. Rev. **B55**, (1997) 12331-12337.
36. B. Wolf, S. Zherlitsyn, S. Schmidt, B. Lüthi, Europhys. Lett. **48**, (1999) 182-186.
37. H.B. Weber, T. Werner, J. Wosnitza, H. v. Löhneysen, U. Schotte, Phys. Rev. **B54**, (1996) 15924-15927.
38. U. Schotte, A. Kelnberger, N. Stüsser, J. Phys.: Condensed Matter **10**, (1998) 6391-6404.
39. S. Schmidt, B. Wolf, M. Sieling, S. Zvyagin, I. Kouroudis, B. Lüthi, Solid State Communications **108**, (1998) 509-512.
40. X. Wang, T. Xiang, Phys. Rev. **B56**, (1997) 5061-5064.
41. N. Shibata, J. Phys. Soc. Jpn. **66**, (1997) 2221-2223.
42. M.B. Lepetit, G.M. Pastor, Phys. Rev. **B56**, (1997) 4447-4454.
43. M. Kaulke, I. Peschel, Eur. Phys. J. **B5**, (1998) 727-734.
44. I. Peschel, M. Kaulke, Ö. Legeza, Ann. Physik **8**, (1999) 153-164.
45. K. Okunishi, Y, Hieida, Y. Akutsu, Phys. Rev. **E59**, (1999) R6227-R6230.
46. K. Tandon, private communication.